Neuroradiology (2020) 62:511–518
https://doi.org/10.1007/s00234-019-02348-0

INTERVENTIONAL NEURORADIOLOGY

Are hemodynamics of irregular small carotid-ophthalmic aneurysms different from those of regular ones and large aneurysms based on numerical simulation?

Hailin Wan[1] · Lei Huang[1] · Liang Ge[1] · Yeqing Jiang[1] · Gaohui Li[2] · Xiaochang Leng[2] · Xiaoyuan Feng[1] · Jianping Xiang[2] · Xiaolong Zhang[1]

Received: 22 May 2019 / Accepted: 11 December 2019 / Published online: 10 January 2020

Abstract

Purpose The purpose of this study is to investigate whether hemodynamics of unruptured, irregular small intracranial aneurysms (SIAs) are different from those of regular ones and large intracranial aneurysms (LIAs) in ophthalmic artery segment of internal carotid artery (ICA).

Methods Between April 2015 and June 2018, 106 carotid-ophthalmic artery aneurysms were retrospectively analyzed using 3D angiographic images and computational fluid dynamics (CFD). Three categories were stratified: regular SIAs, irregular SIAs and LIAs. Statistical comparisons of the differences in clinical, morphological and hemodynamic parameters among regular SIA, irregular SIA and LIA groups were performed by one-way analysis of variance (ANOVA) or Kruskal–Wallis Test.

Results The median maximal height of regular SIA, irregular SIA and LIA were 3.03 (interquartile range: 2.49–4.22) mm, 4.59 (interquartile range: 3.86–5.32) mm and 11.06 (interquartile range: 9.28–13.69) mm, all $P < 0.05$). Low shear-stress area percentage (LSA%) and oscillatory shear index (OSI) of irregular SIAs and LIAs were not significantly different ($P = 0.72$, $P = 0.27$ respectively), and were significantly higher than those of regular SIAs (all $P < 0.01$). Wall shear stress (WSS) and normalized wall shear stress (NWSS) of irregular SIAs were significantly higher than those of LIAs ($P < 0.01$, $P < 0.01$ respectively), but lower than those of regular SIAs ($P < 0.01$, $P < 0.01$ respectively).

Conclusions Special unruptured irregular SIAs share a similarity of hemodynamic characteristics with LIAs in high LSA% and high OSI, and are different from regular SIAs in hemodynamics.

Keywords Hemodynamics · Morphology · Small intracranial aneurysms · Wall shear stress · Rupture

introduction

Aneurysm size was the most widely used metric for assessing intracranial aneurysm rupture risk.[1] The International Study of Unruptured Intracranial Aneurysms (ISUIA) found that the estimated risk of aneurysm rupture increased with aneurysm size, suggesting that small intracranial aneurysms were least likely to rupture.[2] However, recent studies have increasingly shown that many ruptured aneurysms are small,[3, 4] which poses a treatment dilemma for small aneurysms. In contrast, large aneurysm is traditionally believed to bear a high rupture risk, and intervention is usually necessary.[2, 5] Consequently, shape-based morphological metrics are being explored in latest investigations, with complex shapes apparently correlated with rupture status.[6, 7] Meanwhile, intra-aneurysmal hemodynamic factors, such as wall shear stress (WSS), and oscillatory shear index (OSI), have been proposed as aneurysm rupture indicators.[8–10] Many retrospective studies focused on ruptured aneurysms to discriminate the rupture risk factors. However, rupture might significantly alter aneurysm geometry.[11, 12] Therefore, it might be better to analyze unruptured aneurysms. In addition, aneurysm rupture risk may be different depending on the location and whether the aneurysm is a bifurcation or sidewall aneurysm.[13] Based on these observations, in current

HW and LH contributed equally to this work.

✉ Xiaolong Zhang
xiaolongzhang@fudan.edu.cn

[1] Department of Radiology, Huashan Hospital, Fudan University, No. 12 Middle Wulumuqi Road, Shanghai 200040, China

[2] ArteryFlow Technology Co., Ltd, 459 Qianmo Road, Hangzhou 310051, China

study we choose location-specific unruptured, carotid-ophthalmic artery aneurysms, to investigate whether hemodynamics of irregular small aneurysms are similar to large aneurysms and not to regular small aneurysms.

Material and methods

This retrospective study was approved by the institutional review board, with the requirement for informed patient consent waived. Three-dimensional angiographic images of patients with aneurysms that were diagnosed or treated from April 2015 to June 2018 at our center were reviewed. All collected images were examined for suitability to be included in the study. Only cases in which the 3D images were of sufficient quality for accurate segmentation were included in this study, while ruptured or recurrent endovascular embolization or surgical clipping cases were excluded. Consequently, 94 patients with 106 carotid-ophthalmic artery aneurysms met these criteria and were enrolled in this study. All three-dimensional aneurysm geometries were reconstructed from digital subtraction angiographic (DSA) images with the resolution of 0.2 mm × 0.2 mm × 0.2 mm. In this study aneurysm size was categorized as small (<7 mm) or large (≥ 7 mm). According to the regularity in shape, small aneurysms were divided into irregular and regular groups. Aneurysms with bi- or multi-lobes, daughter sacs or blebs, or other types of wall protrusions on 3D images were considered irregular ones.[14, 15]

Morphological parameters calculations

Morphology-based metrics, including aneurysm maximum height (MH), perpendicular height (PH), neck diameter (ND), bottleneck diameter (BD), parent artery diameter (PAD), bottleneck factor (BF), aspect ratio (AR), size ratio (SR), undulation index (UI), non-sphericity index (NSI), and ellipticity index (EI), were calculated from 3D angiographic images that were acquired and reconstructed as in a previous study.[16]

Computational fluid dynamics (CFD) modeling

Each 3D aneurysm geometry model was imported and meshed using Star-CCM+ (CD Adapco, Melville, NY, USA) to create around 1 million polyhedral elements with a maximum mesh size of 0.1 mm and four layers of wall prism elements for accurate boundary layer resolution. The incompressible Navier-Stokes equations were solved numerically under pulsatile flow conditions using Star-CCM+ (CD Adapco, Melville, NY, USA). The pulsed mean flow rate of 4.6 mL/s was used as inlet boundary condition since all computational models started from internal carotid artery (ICA).[17] The pulsatile velocity waveform was obtained from previous studies.[8] Traction-free boundary conditions were implemented at each outlet and the mass flow rate through each outlet artery was proportional to the cube of its diameter, based on the principle of optimal work.[18] Since the Newtonian effect is negligible in main cerebral vessels, in this study blood was modeled as a Newtonian fluid with a density of 1056 kg/m^3 and a viscosity of 0.0035 N s/m^2. A rigid-wall and no-slip boundary condition was implemented at each vessel wall.

Three pulsatile cycles were simulated to ensure that numerical stability was achieved, and the simulation results from the last cycle was taken as the output. All data presented are the time averages over the third pulsatile cycle of flow simulation. The detailed computational fluid dynamics modeling methods were described previously.[8]

Hemodynamic parameters calculations

From the simulated flow fields, we calculated the following hemodynamic parameters: average parent artery wall shear stress (WSS), average intra-aneurysmal WSS, normalized average intra-aneurysmal WSS (NWSS), low shear-stress area percentage (LSA%), and oscillatory shear index (OSI). NWSS was defined as the average intra-aneurysmal WSS divided by the mean PAWSS.[8] LSA%, defined as the percentage of areas of the aneurysm wall exposed to a WSS below 10% of the mean parent arterial WSS.[19]

Statistical analysis

Normally distributed continuous variables were expressed as the mean ± SD and continuous variables with non-normal distribution were presented as median (interquartile range: 25th quartile to 75th quartile). Categorical data were expressed as frequency and percentage for description. Two groups were compared with an unpaired Student t test or Mann Whitney U test when the variance was heterogeneous or either group exhibited a non-normal distribution. Statistical comparisons of the differences in clinical, morphological and hemodynamic parameters among regular small aneurysms, irregular small aneurysm and large aneurysm groups were performed by a one-way analysis of variance (ANOVA) or Kruskal–Wallis Test when appropriate. Statistical analysis of categorical variables was performed using the chi-square test. In addition, Bonferroni-corrected post hoc test was conducted to adjust the observed significant level for multiple comparisons if the null hypothesis was rejected. A p value of less than 0.05 was considered statistically significant. All analyses were conducted using IBM SPSS statistics for Windows, Version 19.0 (IBM Corp, Armonk, NY, USA).

Results

Patient and aneurysm characteristics

The clinical characteristics of patients between regular small aneurysms, irregular small aneurysms and large aneurysms are shown in Table 1. The cohort consisted of 94 patients with 106 carotid-ophthalmic artery aneurysms (60 regular small aneurysms, 18 irregular small aneurysms, and 28 large aneurysms). The mean age (60.50 ± 7.55 years) of large aneurysm group was not significantly older than that (55.35 ± 10.22 years) of regular small aneurysm group ($P = 0.05$), and was significantly different from that (54.69 ± 8.14 years) of irregular small aneurysm group ($P = 0.03$). Female sex, hypertension, smoking, diabetes mellitus, alcohol abuse and multiple aneurysms were not significantly different among the three groups (all $P > 0.05$).

Patient and aneurysm characteristics

Except parent artery diameter was normally distributed, other morphological parameters were not in normal distribution. The morphological parameters of the three groups were presented in Table 2. Among the three groups, diameters of the parent artery were not significantly different ($P = 0.14$), and the other parameters were significantly different (all $P < 0.01$). The parent artery diameter and undulation index between the irregular small aneurysms and large aneurysms were not significantly different ($P = 0.64$, $P = 0.72$), while the other morphological parameters were significantly different (all $P < 0.05$). About the differences in the morphological parameters between irregular small aneurysms and regular small aneurysms, parent artery diameter, bottleneck factor, neck diameter, ellipticity index, and non-sphericity index were not significantly different ($P = 0.27$, $P = 0.18$, $P = 0.12$, $P > 0.05$, $P = 0.42$, $P > 0.05$, respectively), while the maximum height, size ratio, perpendicular height, aspect ratio and undulation index were significantly different between irregular small aneurysms and regular small aneurysm (all $P < 0.05$). Two aneurysms (2/28, 7.14%) in large aneurysm group were regular sac.

Hemodynamic characteristics

The hemodynamic parameters of the three groups are presented in Table 3 and all hemodynamic parameters were not normally distributed. The differences in LSA%, oscillatory shear index, WSS and NWSS among the three groups are presented in Fig. 1. The LSA% and OSI between irregular small aneurysms and large aneurysms were not significantly different ($P = 0.72$, $P = 0.27$ respectively), and were significantly higher than those of regular small aneurysm (all $P < 0.01$). wall shear stress and normalized wall shear stress of irregular small aneurysm were significantly higher than those of large aneurysms ($P < 0.01$, $P < 0.01$ respectively), but lower than those of regular small aneurysm ($P < 0.01$, $P < 0.01$, respectively). wall shear stress and normalized wall shear stress of small aneurysm (both regular and irregular) were also higher than those of large aneurysms ($P < 0.01$, $P < 0.01$ respectively), while the LSA% and oscillatory shear index are lower than those of large aneurysms ($P < 0.01$, $P < 0.01$ respectively) (Fig. 2). Three hemodynamic categories were concluded: regular small aneurysm, as controls, with high wall shear stress and normalized wall shear stress and low LSA and oscillatory shear index; irregular small aneurysm, with medium wall shear stress and normalized wall shear stress and high LSA and oscillatory shear index; large aneurysms with low wall shear stress and normalized wall shear stress and high LSA and oscillatory shear index (Fig. 3).

Discussion

This study compared the clinical, morphological and hemodynamic characteristics of unruptured large aneurysms and irregular small aneurysm in the same location using regular small aneurysms as a control group. We observed that irregular small aneurysm with high LSA% and oscillatory shear index shared similar hemodynamics with large aneurysms. Based on the size and regularity in shape, we proposed a new hemodynamic category for sidewall aneurysms: regular

Table 1 The patient clinical characteristics of regular small intracranial aneurysm (RSIA), irregular small intracranial aneurysm (IRSIA) and large intracranial aneurysm (LIA) group

	Patient with RSIA ($n = 52$)	Patient with IRSIA ($n = 16$)	Patient with LIA ($n = 26$)	P Value
Female Sex	40 (76.92%)	11 (68.75%)	23 (88.46%)	0.28
Age (years)	55.35 ± 10.22	54.69 ± 8.14	60.50 ± 7.55	0.06
Hypertension	14 (26.92%)	4 (25.00%)	12 (46.15%)	0.19
DM	5 (9.62%)	0 (0%)	3 (11.54%)	0.39
Alcohol Abuse	1 (1.92%)	2 (12.50%)	0 (0.00%)	0.06
Smoking	5 (9.62%)	5 (31.25%)	2 (7.69%)	0.05
Multiple IAs	9 (17.31%)	5 (31.25%)	3 (11.54%)	0.27

Table 2 Morphologic characteristics of regular small intracranial aneurysm (RSIA), irregular small intracranial aneurysm (IRSIA) and large intracranial aneurysm (LIA) group

	RSIAs ($n = 60$)	IRSIAs ($n = 18$)	LIAs ($n = 28$)	P Value	P Value for multiple comparison		
					RSIAs vs IRSIAs	RSIAs vs LIAs	IRSIAs vs LIAs
MH (mm)	3.03 (2.49–4.22)	4.59 (3.86–5.32)	11.06 (9.28–13.69)	< 0.01	< 0.01	< 0.01	< 0.01
PH (mm)	2.77 (2.24–3.95)	4.00 (3.56–4.75)	10.04 (8.62–12.02)	< 0.01	< 0.01	< 0.01	< 0.01
ND (mm)	4.07 (3.46–4.98)	4.30 (3.75–5.16)	8.61 (5.80–9.60)	< 0.01	1.00	< 0.01	< 0.01
PAD (mm)	3.80 ± 0.58	3.64 ± 0.39	3.56 ± 0.51	0.14	0.27	0.06	0.64
BD (mm)	4.15 (3.62–5.00)	4.78 (4.24–5.32)	11.55 (9.10–14.18)	< 0.01	0.18	< 0.01	< 0.01
BF	0.99 (0.99–1.04)	1.11 (0.99–1.22)	1.47 (1.29–1.63)	0.01	0.03	< 0.01	< 0.01
SR	0.81 (0.65–1.07)	1.19 (1.05–1.47)	3.33 (2.49–4.18)	< 0.01	< 0.01	< 0.01	< 0.01
AR	0.67 (0.57–0.85)	0.95 (0.71–1.18)	1.33 (1.09–1.59)	< 0.01	< 0.01	< 0.01	< 0.01
EI	0.29 (0.27–0.33)	0.27 (0.26–0.30)	0.25 (0.24–0.27)	< 0.01	0.42	< 0.01	< 0.01
NSI	0.30 (0.28–0.35)	0.31 (0.27–0.33)	0.26 (0.25–0.29)	< 0.01	1.00	< 0.01	< 0.01
UI	0.02 (0.02–0.03)	0.05 (0.02–0.10)	0.03 (0.02–0.06)	< 0.01	< 0.01	0.06	0.72

AR indicates aspect ratio; BD, bottleneck diameter; BF, bottleneck factor; EI, ellipticity index; MH, maximum height; ND, neck diameter; PAD, parent artery diameter; PH, perpendicular height; NSI, non-sphericity index; SR, size ratio; UI, undulation index

small aneurysm with high wall shear stress and low LSA% and oscillatory shear index, irregular small aneurysm with medium wall shear stress and high LSA% and oscillatory shear index, large aneurysms with low wall shear stress and high LSA% and oscillatory shear index. With increasing aneurysm size, the wall shear stress tended to decrease, while the LSA% and oscillatory shear index increased.

In morphological aspects, previous studies found that the irregular shape of aneurysms indicated high rupture risk in a large cohort.[14] Furthermore, size ratio, calculated by dividing the aneurysm size by the average parent vessel size, was found as a useful rupture discriminant in previous studies.[16] However, our study found that the size ratio of large aneurysms was larger than those of irregular small aneurysms. Considering that our study focused on the same location, the parent artery diameters of the two groups were not significantly different. Therefore, size ratio was positively correlated with the maximum height of aneurysms. In addition, our study found that the difference in undulation index, capturing the degree of aneurysm surface concavity and quantitatively reflecting the regularity of aneurysms,[16] among the three categories were significantly different. This observation demonstrated quantitatively the reliability of classifying aneurysms as three groups. Furthermore, recent study showed that quantification of hemodynamic irregularity using oscillatory velocity index was associated with the rupture status of intracranial aneurysms.[20] Irregular ruptured aneurysms are more likely to have higher vortex core line length than unruptured ones.[21]

Previous studies suggested that aneurysms with different size ranges tended to have different pathophysiological presentations.[22, 23] These data suggested that aneurysm pathophysiological phenotypes existed on a spectrum: at one extreme was the small, thin-walled phenotype; at the other extreme was the large, thick-walled phenotype; in between was a continuum representing an amalgamation of the previous two basic types.[24] Furthermore, the aberrant flow conditions caused by aneurysm geometry were the likely cause of the endothelial dysfunction, which resulting accumulation of cytotoxic and pro-inflammatory substances into the aneurysm

Table 3 Hemodynamic parameters of regular small intracranial aneurysm (RSIA), irregular small intracranial aneurysm (IRSIA) and large intracranial aneurysm (LIA) group

	Regular SIAs (n = 60)	Irregular SIAs (n = 18)	LIAs (n = 28)	P Value
PAWSS (Pa)	8.95 (7.71–11.26)	11.05 (9.67–12.74)	9.48 (7.13–11.21)	0.75
WSS (Pa)	6.27 (4.43–9.32)	4.51 (2.73–5.27)	2.23 (1.78–2.87)	< 0.01
NWSS	0.67 (0.51–0.867)	0.38 (0.31–0.50)	0.23 (0.19–0.32)	< 0.01
LSA%	0.71 (0.23–2.35)	17.06 (12.56–34.35)	25.86 (14.21–37.44)	< 0.01
OSI	0.01 (0.00–0.01)	0.01 (0.01–0.02)	0.02 (0.01–0.03)	< 0.01

LSA, low shear-stress area; NWSS, normalized wall shear stress; OSI, oscillatory shear index; PA WSS, parent artery wall shear stress; WSS, wall shear stress

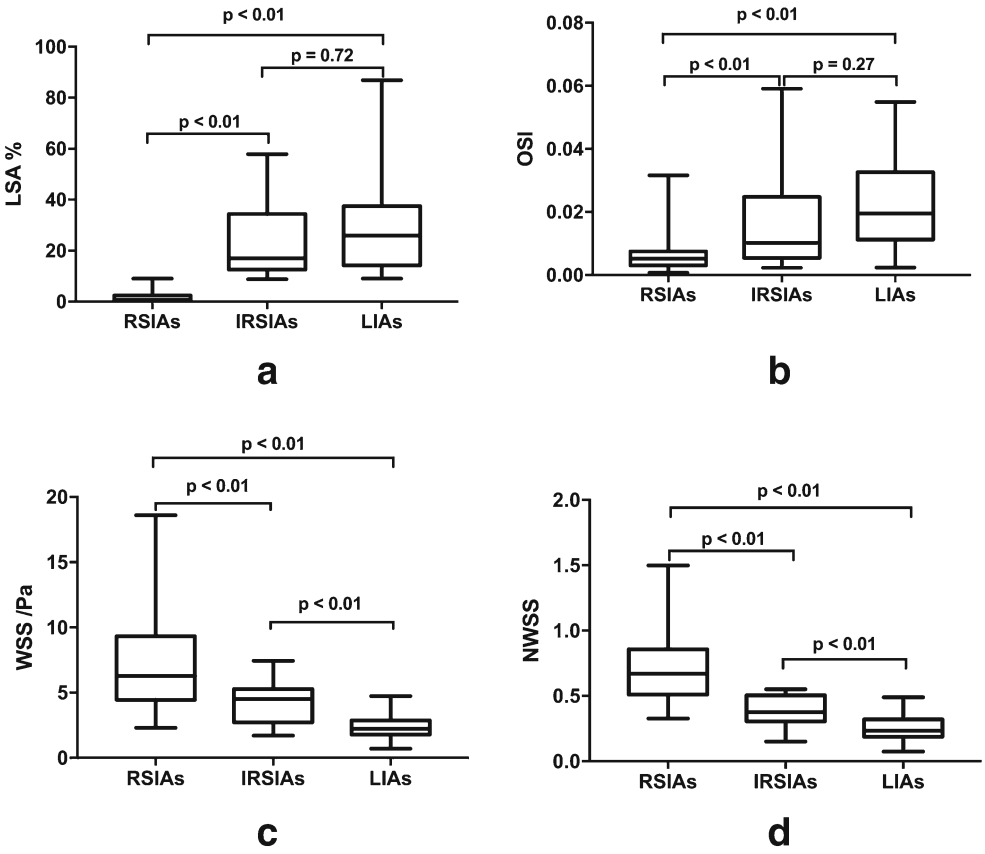

Fig. 1 The differences in LSA% (A), OSI (B), WSS (C) and NWSS (D) among the three IA groups are presented as box plot (median with quartiles). IRSIAs, irregular small intracranial aneurysms; LIAs, large intracranial aneurysms; LSA%, low shear stress area percentage; NWSS, normalized wall shear stress; OSI, oscillatory shear index; RSIAs, regular small intracranial aneurysms

wall. This process could eventually lead to the decellularized and degenerated aneurysm wall which was prone to rupture.[25] Furthermore, Frösen et al. found that histological structure of aneurysm wall did not associate with size, although it did correlate with rupture status.[26] In the current study, although the mean size of irregular carotid-ophthalmic small aneurysms was between those of regular small aneurysms and large aneurysms, the hemodynamic characteristics was significantly different from regular small aneurysms and similar with age aneurysms. We hypothesized that in side-wall aneurysms, a high wall shear stress might facilitate the aneurysm to initiate and grow, while a low wall shear stress might drive the wall to degenerate and rupture when it reached a point of breakout. Furthermore, from local hemodynamics associated with visible focal wall changes intra-operatively, Cebral et al. found that low and oscillatory wall shear stress was associated with atherosclerotic and hyperplastic changes while higher and less oscillatory wall shear stress were associated with local "thinning" of the wall.[27] In this study, small aneurysms presented with higher wall shear stress may have thin wall while large aneurysms with lower wall shear stress may have atherosclerotic and hyperplastic changes in their walls.

Currently, many studies have also demonstrated that higher LSA% and oscillatory shear index are associated with aneurysm rupture status,[8, 28] albeit with conflicting findings regarding wall shear stress.[24] Furthermore, previous studies have observed that the thin-walled dome regions of unruptured aneurysms are co-localized with high wall shear stress, while bleeding points of ruptured aneurysms were often located at the dome of aneurysms with low wall shear stress.[29] In pathobiology, low wall shear stress can cause dysfunction of flow-induced nitric oxide (NO), increase endothelial permeability, and trigger atherosclerotic and inflammatory pathways.[30] Albeit with conflict of wall shear stress for aneurysmal rupture, Cebral et al. revealed that elevated flow activity and high wall shear stress were related to inflammation associated with degenerative wall remodeling and rupture, which is in fact not at all contradictory to current vascular biology knowledge, but rather very much in line with current knowledge on the effect of WSS on vascular remodeling.[31] Varble et al.[28] dichotomized aneurysms into small and large aneurysms using hierarchal cluster analysis and found that in both groups, ruptured aneurysms had higher oscillatory shear index, low shear-stress area (LSA), and lower normalized wall shear stress, than unruptured aneurysms. In bilateral mirror aneurysm models, multiple studies also demonstrated that ruptured aneurysms manifested higher LSA.[32, 33] In the current study, the unruptured large aneurysms and irregular small aneurysms had lower wall shear stress and higher LSA% than those of regular small aneurysms, which might indicate that the irregular small aneurysms and large aneurysms were more prone to rupture.

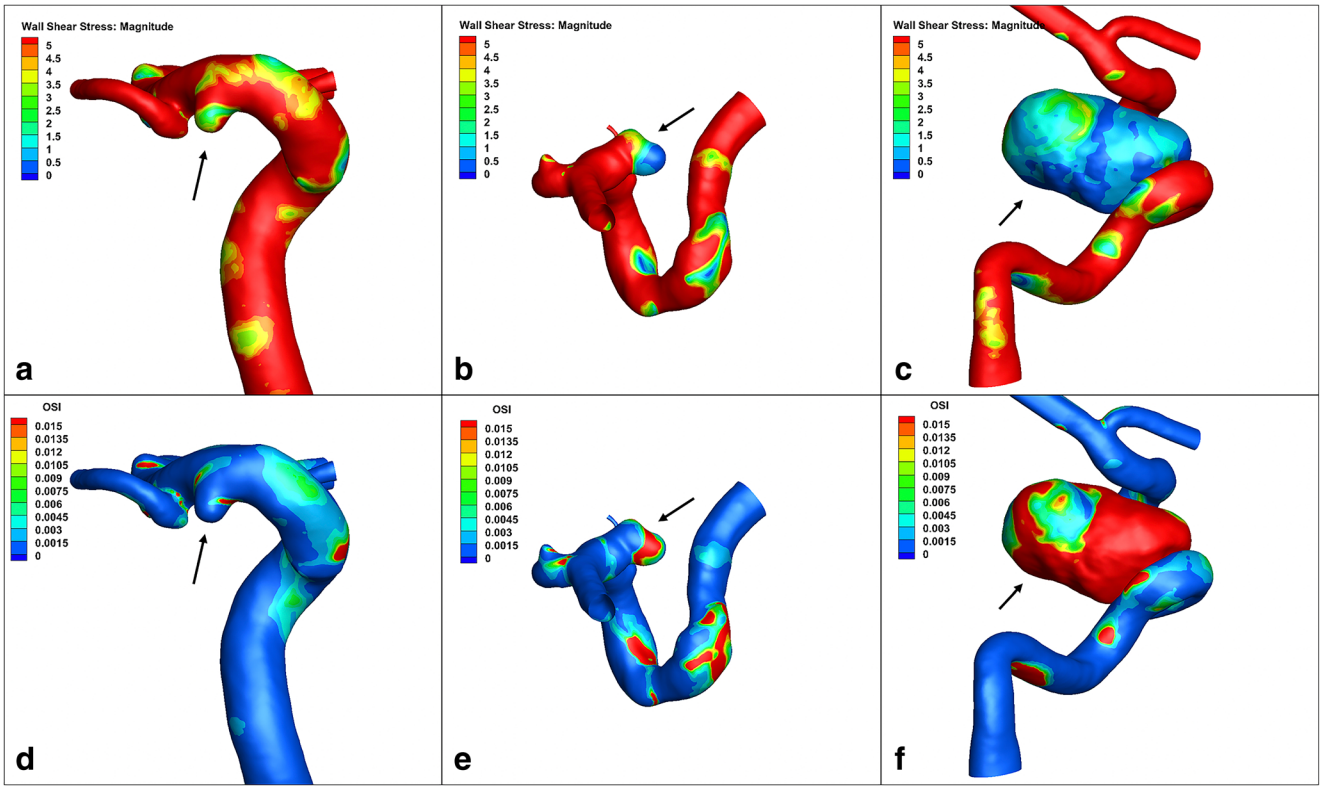

Fig. 2 The WSS magnitude and OSI maps of regular SIAs (A, D), irregular SIAs (B, E), and LIAs (C, F) of three carotid-ophthalmic artery aneurysms reveal that regular SIAs are present as high WSS and low OSI while irregular SIAs and LIAs show as low WSS and high OSI. SIAs, small intracranial aneurysms; LIAs, large intracranial aneurysms; LSA%, low shear stress area percentage; NWSS, normalized wall shear stress; OSI, oscillatory shear index

Previous studies showed that the hemodynamics of sidewall and bifurcation aneurysms might be different.[34, 35] Baharoglu et al.[34] found that the side wall aneurysm model with increasing inflow angle had deeper penetration of flow, higher velocities, and higher wall shear stress inside the aneurysm dome compared with bifurcation model. In addition, in a systematic review and meta-analysis study Can et al.[35] documented that high wall shear stress was positively correlated with the formation and rupture of bifurcation aneurysms, whereas negative correlations were seen in sidewall aneurysms. Our study focused on carotid-ophthalmic artery aneurysms and revealed accordant mean wall shear stress and LSA% with the previous study.[36] So further study can be investigated to aneurysms in other specific sites.

This study has several limitations. First, our patient population is from a single center, and selection bias may exist in this retrospective study. Second, the irregular small aneurysms sample size and proportion (16.98%) are relatively small. Third, we adopted several commonly used assumptions to make computational fluid dynamics tractable. Because of a lack of patient-specific information, we assumed a generic inlet waveform and a constant, location-based inlet flow rate.

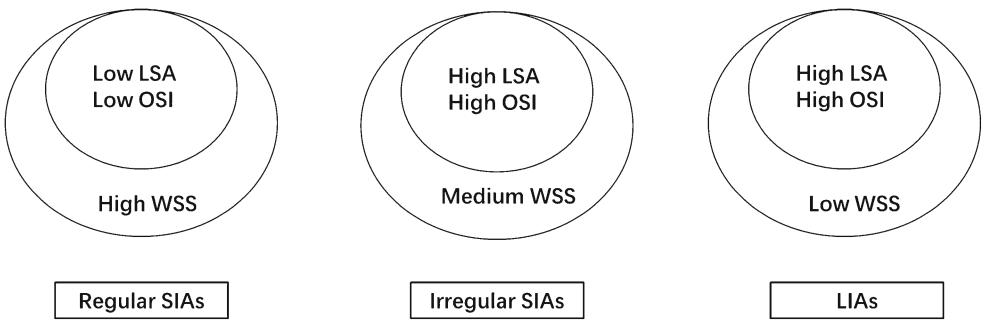

Fig. 3 Three hemodynamic modes: regular SIAs, as controls, with high WSS and NWSS and low LSA and OSI; irregular SIAs, with medium WSS and NWSS and high LSA and OSI; LIAs, with low WSS and NWSS and high LSA and OSI. SIAs, small intracranial aneurysms; LIAs, large intracranial aneurysms; LSA%, low shear stress area percentage; NWSS, normalized wall shear stress; OSI, oscillatory shear index

The inlet velocities were scaled by the inlet diameter. We also assumed blood as a Newtonian fluid and that aneurysms had rigid walls. At last, in this study we applied the planar separation of aneurysm from the parent vessel, which may influence the outcome. For most cases with simple aneurysms the way we isolated the aneurysm should be accurate. However, it may be problematic for wide-neck or complex aneurysms. We could use a curve to segment the aneurysm, but it will be difficult to calculate many morphological parameters since they were defined under the aneurysm isolation using a plane.

Conclusions

Specially unruptured and irregular small aneurysms have similar hemodynamic characteristics with large aneurysms and are different from regular small aneurysms in terms of hemodynamics. This may indicate that these irregular small aneurysms harbor a high risk for growth or rupture and thus need more a close follow-up, compared with regular ones.

Funding information This study was funded by the National Nature Science Foundation of China (Grant Nos. 81771242 and 81371308).

Compliance with ethical standards

Conflict of interest We declare that we have no conflict of interest.

Ethical approval All procedures performed in studies involving human participants were in accordance with the ethical standards of the institutional and/or national research committee and with the 1964 Helsinki declaration and its later amendments or comparable ethical standards. For this type of study formal consent is not required.

Informed consent Informed consent was obtained from all individual participants included in the study.

References

1. Greving JP, Wermer MJ, Brown RD Jr et al (2014) Development of the PHASES score for prediction of risk of rupture of intracranial aneurysms: a pooled analysis of six prospective cohort studies. Lancet Neurol 13:59–66
2. Wiebers DO (2003) Unruptured intracranial aneurysms: natural history, clinical outcome, and risks of surgical and endovascular treatment. Lancet 362:103–110
3. Lee GJ, Eom KS, Lee C, Kim DW, Kang SD (2015) Rupture of very small intracranial aneurysms: incidence and clinical characteristics. J Cerebrovasc Endovasc Neurosurg 17:217–222
4. Nahed BV, DiLuna ML, Morgan T et al (2005) Hypertension, age, and location predict rupture of small intracranial aneurysms. Neurosurgery 57:676–683
5. Juvela S, Poussa K, Lehto H, Porras M (2013) Natural history of unruptured intracranial aneurysms: a long-term follow-up study. Stroke 44:2414–2421
6. Ujiie H, Tamano Y, Sasaki K, Hori T. (2001)Is the aspect ratio a reliable index for predicting the rupture of a saccular aneurysm? Neurosurgery 48:495-502; discussion 502-493
7. Kashiwazaki D, Kuroda S (2013) Size ratio Can highly predict rupture risk in intracranial small (<5 mm) aneurysms. Stroke 44: 2169–2173
8. Xiang J, Natarajan SK, Tremmel M, Ma D, Mocco J, Hopkins LN, Siddiqui AH, Levy EI, Meng H (2011) Hemodynamic–morphologic discriminants for intracranial aneurysm rupture. Stroke 42:144–152
9. Boussel L, Rayz V, McCulloch C, Martin A, Acevedo-Bolton G, Lawton M, Higashida R, Smith WS, Young WL, Saloner D (2008) Aneurysm growth occurs at region of low wall shear stress: patient-specific correlation of hemodynamics and growth in a longitudinal study. Stroke 39:2997–3002
10. Cebral JR, Castro MA, Burgess JE, Pergolizzi RS, Sheridan MJ, Putman CM (2005) Characterization of cerebral aneurysms for assessing risk of rupture by using patient-specific computational hemodynamics models. AJNR Am J Neuroradiol 26:2550–2559
11. Rahman M, Ogilvy CS, Zipfel GJ et al (2011) Unruptured cerebral aneurysms do not shrink when they rupture: multicenter collaborative aneurysm study group. Neurosurgery 68:155–160
12. Schneiders JJ, Marquering HA, van den Berg R, VanBavel E, Velthuis B, Rinkel GJ, Majoie CB (2014) Rupture-associated changes of cerebral aneurysm geometry: high-resolution 3D imaging before and after rupture. Am J Neuroradiol 35:1358–1362
13. Zhang Y, Tian Z, Jing L, Zhang Y, Liu J, Yang X (2016) Bifurcation Type and Larger Low Shear Area Are Associated with Rupture Status of Very Small Intracranial Aneurysms Frontiers in Neurology:7
14. Lindgren AE, Koivisto T, Bjorkman J et al (2016) Irregular shape of intracranial aneurysm indicates rupture risk irrespective of size in a population-based cohort. Stroke 47:1219–1226
15. Björkman J, Frösen J, Tähtinen O, Backes D, Huttunen T, Harju J, Huttunen J, Kurki MI, von Und Zu Fraunberg M, Koivisto T, Manninen H, Jääskeläinen JE, Lindgren AE (2017) Irregular shape identifies ruptured intracranial aneurysm in subarachnoid hemorrhage patients with multiple aneurysms. Stroke 48:1986–1989
16. Dhar S, Tremmel M, Mocco J et al (2008) Morphology parameters for intracranial aneurysm rupture risk assessment. Neurosurgery 63: 185–197
17. Fahrig R, Nikolov H, Fox AJ, Holdsworth DW. (1999)A three-dimensional cerebrovascular flow phantom. Medical physics 26: 1589-1599
18. Oka S, Nakai M (1987) Optimality principle in vascular bifurcation. Biorheology 24:737–751
19. Jou LD, Lee DH, Morsi H, Mawad ME (2008) Wall shear stress on ruptured and unruptured intracranial aneurysms at the internal carotid artery. AJNR Am J Neuroradiol 29:1761–1767
20. Tanioka S, Ishida F, Kishimoto T, et al. (2019)Quantification of hemodynamic irregularity using oscillatory velocity index in the associations with the rupture status of cerebral aneurysms. Journal of NeuroInterventional Surgery
21. Byrne G, Mut F, Cebral J (2014) Quantifying the large-scale hemodynamics of intracranial aneurysms. AJNR Am J Neuroradiol 35: 333–338
22. Kadasi LM, Dent WC, Malek AM. (2013)Cerebral aneurysm wall thickness analysis using intraoperative microscopy: effect of size and gender on thin translucent regions. J Neurointerv Surg 2013;5: 201–206
23. Kataoka K, Taneda M, Asai T, Yamada Y (2000) Difference in nature of ruptured and unruptured cerebral aneurysms The Lancet:355
24. Meng H, Tutino VM, Xiang J, Siddiqui A (2014) High WSS or low WSS? Complex interactions of hemodynamics with intracranial

aneurysm initiation, growth, and rupture: toward a unifying hypothesis. AJNR Am J Neuroradiol 35:1254–1262
25. Frosen J, Tulamo R, Paetau A et al (2012) Saccular intracranial aneurysm: pathology and mechanisms. Acta Neuropathol 123: 773–786
26. Frösen J, Piippo A, Paetau A, Kangasniemi M, Niemelä M, Hernesniemi J, Jääskeläinen J (2004) Remodeling of Saccular cerebral artery Aneurysm Wall is associated with rupture. Stroke 35: 2287–2293
27. Cebral JR, Detmer F, Chung BJ et al (2019) Local hemodynamic conditions associated with focal changes in the intracranial Aneurysm Wall. AJNR Am J Neuroradiol 40:510–516
28. Varble N, Tutino VM, Yu J, Sonig A, Siddiqui AH, Davies JM, Meng H (2018) Shared and distinct rupture discriminants of small and large intracranial aneurysms. Stroke 49:856–864
29. Omodaka S, Sugiyama S, Inoue T, Funamoto K, Fujimura M, Shimizu H, Hayase T, Takahashi A, Tominaga T (2012) Local hemodynamics at the rupture point of cerebral aneurysms determined by computational fluid dynamics analysis. Cerebrovasc Dis 34:121–129
30. Malek AM, Alper SL, Izumo S (1999) Hemodynamic shear stress and its role in atherosclerosis. JAMA 282:2035–2042
31. Cebral J, Ollikainen E, Chung BJ, Mut F, Sippola V, Jahromi BR, Tulamo R, Hernesniemi J, Niemelä M, Robertson A, Frösen J (2017) Flow conditions in the intracranial aneurysm lumen are associated with inflammation and degenerative changes of the Aneurysm Wall. AJNR Am J Neuroradiol 38:119–126
32. Lu G, Huang L, Zhang XL, Wang SZ, Hong Y, Hu Z, Geng DY (2011) Influence of hemodynamic factors on rupture of intracranial aneurysms: patient-specific 3D mirror aneurysms model computational fluid dynamics simulation. AJNR Am J Neuroradiol 32: 1255–1261
33. Fan J, Wang Y, Liu J, et al. (2015)Morphological-hemodynamic characteristics of intracranial bifurcation Mirror aneurysms. World neurosurgery 84:114-120.e112
34. Baharoglu MI, Lauric A, Gao BL, Malek AM (2012) Identification of a dichotomy in morphological predictors of rupture status between sidewall- and bifurcation-type intracranial aneurysms. J Neurosurg 116:871–881
35. Can A, Du R (2016) Association of Hemodynamic Factors with Intracranial Aneurysm Formation and Rupture: systematic review and meta-analysis. Neurosurgery 78:510–520
36. Varble N, Rajabzadeh-Oghaz H, Wang J, Siddiqui A, Meng H, Mowla A (2017) Differences in morphologic and hemodynamic characteristics for "PHASES-based" intracranial aneurysm locations. AJNR Am J Neuroradiol 38:2105–2110